Jia, Wenlong; Lin, Youzhi; Yang, Fan; Li, Changjun

Article

A novel lift-off diameter model for boiling bubbles in natural gas liquids transmission pipelines

Energy Reports

Provided in Cooperation with:
Elsevier

Suggested Citation: Jia, Wenlong; Lin, Youzhi; Yang, Fan; Li, Changjun (2020) : A novel lift-off diameter model for boiling bubbles in natural gas liquids transmission pipelines, Energy Reports, ISSN 2352-4847, Elsevier, Amsterdam, Vol. 6, pp. 478-489, https://doi.org/10.1016/j.egyr.2020.02.014

Energy Reports 6 (2020) 478–489

Contents lists available at ScienceDirect

Energy Reports

journal homepage: www.elsevier.com/locate/egyr

Research paper

A novel lift-off diameter model for boiling bubbles in natural gas liquids transmission pipelines

Wenlong Jia *, Youzhi Lin, Fan Yang, Changjun Li

School of Petroleum Engineering, Southwest Petroleum University, Chengdu, 610500, China

ARTICLE INFO

Article history:
Received 4 November 2019
Received in revised form 16 February 2020
Accepted 19 February 2020
Available online xxxx

Keywords:
Natural gas liquids
Pipe
Boiling flow
Bubble
Lift-off diameter

ABSTRACT

The pipeline is a convenient and safe way to transport natural gas liquids (NGLs). However, the NGL is easy to boil due to the variations of pressures and temperatures along the pipeline. The bubble lift-off diameter is an essential parameter to calculate the mass and heat transfer rates between vapor and liquid phases for the NGL two-phase saturated boiling flow. This paper proposed a novel bubble lift-off diameter model based on the force-balance principle of bubbles, which considers the effects of the pressure, shear lift force, unstable drag force, surface tension, gravity force, buoyancy force, gas-phase density, bubble volume, bubble flow velocity, and bubble growth time on the bubble's lift-off diameters at various pipe inclination angles. A total of 136 experimental data points are applied to validate the new model. Results demonstrate that the average relative deviation (ARD) between the experimental bubble's lift-off diameters and calculated values based on the new model is in the range from 5.75% to 29.95%. In contrast, for horizontal and vertical pipes, the minimum ARDs of seven existing models (Fritz, Kocamustaf, Zeng, Lee, Situ, Hamzekhani, Chen models) are in the range from 19.42% to 42.58%, respectively. Moreover, the in-depth force analysis results reveal that the shear lift force, buoyancy force, drag force and surface tension force are dominant factors affecting the bubble lift-off diameters in inclined pipes. The new model provides an effective method to calculate the bubble lift-off diameter in the pipe at various inclination angles, overcoming the deficiencies of most existing models that only can be applied to either horizontal or vertical pipes.

1. Introduction

Natural Gas Liquids (NGLs) primarily contain several light hydrocarbon components (ethane, propane, isobutane and natural gasoline) that are produced in conjunction with raw natural gas, shale gas, and condensate gas or as a byproduct of the crude oil refining process (Jia et al., 2017; Wang et al., 2018). NGLs are more valuable than the dry natural gas in terms of the sale prices, so it is profitable to refine NGL components from natural gas. It is predicted that the NGL production amounts would reach 3 million barrels per day by 2025 in the USA owing to the rapid development of shale gas (Stevens, 2012).

The pipeline is a convenient and safe way to transport large amounts of NGL from gas fields/refiners to end consumers. In order to enhance the pipeline transportation efficiency and to save transportation energy consumption, the NGL pipeline should be operated at a specified pressure and temperature range to keep the NGL staying in the liquid phase (Jia et al., 2017). However, the dynamic pressure and temperature variations are inevitable because of unsteady operation and heat transfer processes, such as the valve closing/opening, pump startup/shutdown cases, and the heat transfer from the high-temperature air to pipes in summer (Jia et al., 2020).

Decreasing or increasing the pressure may further cause the evaporation of the liquids, resulting in the vapor–liquid two-phase flow in the pipe because the pressure and temperature are critical parameters to determine the phase state of the NGL (Chen et al., 2012; Jia et al., 2017). Such an evaporation phenomenon is also known as the liquid boiling that is featured by the bubble generation and lift-off processes on the inner wall of the pipe (Chen et al., 2004; Cho et al., 2011; Gong et al., 2013). The bubble's lift diameter is an essential parameter for the calculation of the evaporation rate and heat transfer rate between vapor and liquid phases (Kirichenko, 1973; Kirichenko et al., 1976; Kocamustaf and Ishii, 1983; Jia et al., 2017). Many achievements and mathematical models have already involved in the calculation of the lift-off diameters of bubbles (Shao et al., 2011), which can be generally classified into two types: the empirical-correlation method and the theoretical model.

The empirical model was built by fitting large amounts of experimental data. Fritz (1935) firstly proposed a correlation to calculate the bubble departure diameter by building the force-balance relationship between the buoyancy force and surface

* Corresponding author.
E-mail address: jiawenlongswpu@hotmail.com (W. Jia).

https://doi.org/10.1016/j.egyr.2020.02.014

Nomenclature

b	bubble growth constant
d_b	bubble diameter
d_w	contact diameter (m)
d_l	bubble lift-off diameter
g	gravity acceleration
Ja	Jakob Number
P	pressure
q	heat flux
Re	Reynolds number
T	temperature
u	velocity
t	time

Greek letters

α	pipe inclination angle
ρ	density
θ	contact angle

Subscripts

a	advancing
l	liquid phase
r	receding
y	force component on y-axis
g	vapor phase

tension force. The Fritz model is then taken as the basement to build both of the empirical models and theoretical models. Zuber (1959) presented that the boiling bubble formation process on the horizontal surface was similar to that at the orifice, so the bubble diameter detached from the heated horizontal surface was related to the radius of the active nucleation site. Cole and Rohsenow (1969) correlated experimental results obtained from pool boiling experiments of water and organic liquids at both atmospheric and sub-atmospheric pressures. They found that the bubble departure diameter was affected by the bubble growth rate as well as the buoyancy force and surface tension force. Kocamustaf and Ishii (1983) observed that the Fritz model was accurate when the pressure was close to atmospheric pressure. For the high-pressure boiling process, they proposed a modified equation that contains a system pressure-related correction term. Lee et al. (2003) applied the Rayleigh method to analyze the dimension of the bubble growth rate of R11 and R113 refrigerants in a horizontal boiling pool at the normal pressure. They proposed a function that depicts the relationship between the bubble lift-off diameter and Jakob Number of refrigerants. Kim and Kim (2006) built a bubble lift-off diameter model at low-pressure based on fitting a large number of experimental data regarding water and refrigerant boiling processes. Chen et al. (2018) developed a bubble lift-off diameter model suitable for high-pressure ethane based on vertical pool boiling experiments and on fitting the experimental data. These empirical correlations have considerable accuracy when the fluid composition, the pressures, and temperatures fall in the ranges of the experimental conditions. However, it is difficult to extend these correlations to the conditions beyond the original experimental pressure, temperature, and fluid composition ranges.

The theoretical model was generally built based on the force-balance principle of the bubble. Fritz (1935) presented a lift-off diameter model for the horizontal pool boiling based on the force-balance, including the buoyancy and surface tension forces.

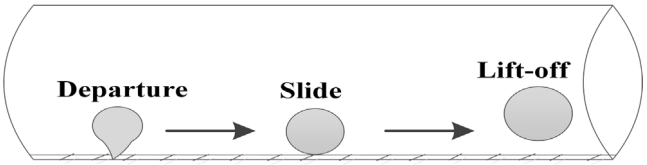

Fig. 1. The Bubble formation process for NGL boiling flow in pipes.

Kirichenko et al. (1976) considered the effects of the wall shear force on the bubble's lift-off process, yielding a bubble lift-off diameter model for horizontal pipes. Klausner et al. (1993) investigated the bubble departure in the nucleate boiling flow. They confirmed that the major forces acting on bubbles are the surface tension force, the unsteady drag forces related to the bubble growth, the shear lift force related to the velocity gradient close to the wall, the buoyancy force, and a contact pressure force arising from the pressure difference between a bubble and the surrounding liquid. Situ et al. (2005) built a bubble lift-off diameter model for a vertical boiling flow pipe according to the force-balance between the bubble's unstable drag force and shear lift force. Recently, Colombo and Fairweather (2015) modified the Klausner method (Klausner et al., 1993) by using a new surface tension force model and considering the effects of the microlayer evaporation on the bubble growth process, yielding reasonable agreement between calculations and experimental bubble departure diameters in subcooled and saturated forced convective boiling flow. These mentioned models were mainly built for the pool boiling process, vertical pipe or horizontal pipe flow. Also, most of these models neglected the effects of gas–liquid velocity difference on the bubble lift-off diameter.

Existing models are difficult to accurately calculate the bubble lift-off diameter of NGLs in pipes with various inclinations. In what follows, this paper proposed a bubble lift-off diameter model suitable for pipes with various inclined angles based on the force-balance principle. The forces incorporated in the new model included the unstable resistance force, shear lift force, buoyancy force as well as the effect of gas–liquid velocity difference. Finally, the new model was validated with various data.

2. The lift-off process of NGL bubble in flow boiling

When the pressure of the NGL pipeline suddenly decreases under unstable operation conditions, the NGL temperature will be higher than its saturation temperature, resulting in the evaporation of the NGL (Jia et al., 2017). Such an evaporation process is also known as the boiling flow dominated by the bubble formation process, which is composed of three subsequent stages as shown in Fig. 1, namely the bubble generation stage, the bubble slide stage, and the bubble lift-off stage (Faraji et al., 1994; Situ et al., 2005; Torregrosa et al., 2016). The key parameters used to describe the bubble in the above three stages include the bubble departure diameter, bubble departure frequency, bubble lift-off diameter, and the active nucleation density (Klausner et al., 1993; Gong et al., 2013). The bubble departure diameter here refers to the bubble diameter at the time when the bubble departs from the active nucleation and starts to slide on the heated wall. Likewise, the bubble lift-off diameter indicates the diameter of the bubble when it detaches from the pipe inner wall or heated wall. The bubble generated on a special active nucleation site slides on the heated wall in the priority of detaching from it. During the bubble sliding period, the bubble gradually grows up before the diameter reaches its maximum value. So, the bubble departure diameter is relatively smaller than the bubble the lift-off diameter somehow.

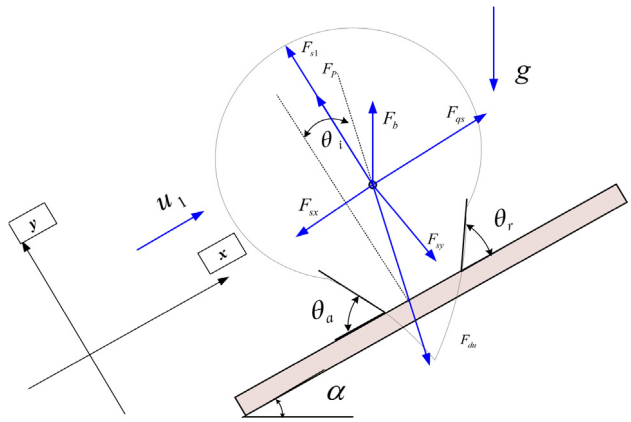

Fig. 2. The force balance analysis of a bubble on the inclined pipe wall. F_p, F_{sl}, F_{du}, F_{sx}, F_{sy}, F_g, F_b, u_1, t refer to the pressure, shear lift force, unstable drag force, surface tension on x-direction, surface tension on y-direction, gravity force, buoyancy force, fluid flow velocity, bubble growth time respectively; θ_r is the bubble receding contact angle; θ_a is the bubble advancing contact angle; α is the pipe's inclination angle; θ_i is the bubble inclined angle, which is the angle between the y-axis and the line from active nucleation site to the center of bubble.

3. Mathematical model

3.1. New bubble lift-off diameter model

Klausner et al. (1993) simplified the forces acting on the bubble attached to the heated surface. Zeng et al. (1993) extended the Klausner model (Klausner et al., 1993) to both pool boiling and flowing boiling processes. These achievements show the feasibility of developing the bubble lift-off diameter model based on the force-balance principle. In this subsection, the force-balance principle is applied to develop the new bubble lift-off diameter model for incline NGL pipes. The shape of the growing bubble is assumed to be a sphere. The forces acting on a boiling bubble include the fluid pressure, buoyancy force, shear lift force, gravity force, unstable resistance force, and surface tension force (Klausner et al., 1993). All forces acting on the bubble can be decomposed into two-component forces in horizontal and vertical directions. The horizontal force (x-axis in Fig. 2) is parallel to the axis of the pipe, and the vertical force (y-axis in Fig. 2) is perpendicular to the axis of the pipe.

Klausner et al. (1993) presented that the summations of forces in the x and y direction must satisfy the condition $\sum F \leq 0$ when the bubble keeps staying on the nucleation site. Once the summation of the forces in the x-direction violates the condition $\sum F \leq 0$, the bubble will slide along the heated wall. On the other hand, if the summation of forces in the y-direction is greater than zero, the bubble will departure from the heated wall. So the lift-off diameter of the bubble is dependent on the forces acting on the y-direction. According to the force decomposition method, the summation of vertical forces acting on the bubble can be calculated from Eq. (1).

$$\sum F_y = F_p + F_{sl} + F_{duy} + F_{sy} + F_{gy} + F_{by} = \rho_g V_b \frac{du_{gy}}{dt} \tag{1}$$

where F_p, F_{sl}, F_{du}, F_s, F_g, F_b, ρ_g, V_b, u_g, and t refer to the pressure, shear lift force, unstable drag force, surface tension, gravity force, buoyancy force, gas-phase density, bubble volume, bubble flow velocity, bubble growth time respectively. Subscript y indicates the y-direction shown in Fig. 2. The bubble will detach from the heated wall once the summation of the forces in the y-direction is higher than zero. All forces acting on the bubble are calculated from the following equations.

3.1.1. Pressure (F_P)

The total pressure acting on a bubble can be divided into two parts: the hydrodynamic pressure F_h and the contacting pressure F_{cp} on the wall. The hydrodynamic pressure originates from hydrodynamic pressure. The contacting pressure force is caused by the pressure difference between the inside and outside of the bubble. These two pressures are expressed by Eqs. (2) and (3).

$$F_h = \frac{9}{8}\rho_l u_r^2 \frac{\pi d_w^2}{4} \tag{2}$$

$$F_{cp} = \frac{2\sigma}{R_{top}} \frac{\pi d_w^2}{4} \tag{3}$$

According to these pressures, the total pressure model for a bubble is given by Eq. (4) (Klausner et al., 1993).

$$F_p = \left[\frac{9}{8}\rho_l u_r^2 + \frac{2\sigma}{R_{top}}\right] \frac{\pi d_w^2}{4} \tag{4}$$

where ρ_l, u_r, σ refer to the liquid-phase density, relative velocity, surface tension coefficient, respectively. R_{top} denotes curvature radius at the top of the bubble, usually ranging from d_b to $2.5d_b$. Klausner et al. (1993) suggested $R_{top} = 2.5d_b$. d_w is the bubble-heated wall contact diameter

3.1.2. Buoyancy force (F_{by})

The buoyancy force is applied to a bubble in the opposite direction of gravitational acceleration. The buoyancy force on the vertical direction is calculated from Eq. (5) as follows:

$$F_{by} = \frac{1}{6}\pi d_b^3 \rho_l g \cos\alpha \tag{5}$$

where α is the pipe's inclination angle.

3.1.3. Gravity force (F_{gy})

The gravity force on the vertical direction is given by Eq. (6).

$$F_{gy} = \frac{1}{6}\pi d_b^3 \rho_g g \cos\alpha \tag{6}$$

where α is the pipe's inclination angle.

3.1.4. Shear lift force (F_{sl})

This direction of the shear lift force is perpendicular to the pipe axis. It tends to take the bubble away from the wall. Saffman (1965) firstly presented the method to calculate the shear lift force acting on a sphere with a low Rayleigh number. Mei and Klausner (1994) modified the Saffman model (Saffman, 1965) and proposed a relationship based on the assumption of a spherical bubble in an infinite flow field at low Reynolds numbers, as expressed by Eq. (7).

$$F_{sl} = \frac{1}{8} C_{sl} \rho_l u_r^2 \pi d_b^2 \tag{7}$$

where C_{sl} is the shear lift coefficient given by Eq. (8); u_r is the relative velocity between the vapor phase and the liquid phase, $u_r = u_g - u_l$. Situ et al. (2005) proposed a correlation $u_r = 0.5u_g$.

$$C_{sl} = 3.877 G_s^{0.5} \left(Re_b^{-2} + 0.014 G_s^2\right)^{0.25} \tag{8}$$

where G_s is a dimensionless shear rate of oncoming flow of bubble shown in Eq. (9). Re_b is the Rayleigh number given by Eq. (10).

$$G_s = \frac{1}{2}\left|\frac{du_l}{dx}\right| \frac{d_b}{u_r} \tag{9}$$

$$\mathrm{Re}_b = \frac{d_b u_r}{\upsilon_l} \tag{10}$$

3.1.5. Unstable drag force (F_{du})

The asymmetrical growth of the bubble will lead to the unstable drag force which can be taken as the inertial force produced by the mass growth. Klausner et al. (1993) proposed an unstable drag force model for bubbles in cohesionless liquids. Cho et al. (2011) introduced an empirical constant into the Klausner model, resulting in a more comprehensive drag force model as follows:

$$F_{du} = -\frac{1}{16}\rho\pi d^2(t)\left(\frac{3}{2}C_s\dot{d}^2(t) + d(t)\ddot{d}(t)\right) \tag{11}$$

Reorganizing Eq. (12) yields,

$$F_{du} = -\frac{1}{8}\rho\pi d^2(t)\left(\frac{3}{2}C_s\dot{d}^2(t) + d(t)\ddot{d}(t)\right) \tag{12}$$

where $\dot{d}$ is the first derivative of the bubble diameter with respect to the bubble growth time; $\ddot{d}$ is the second derivative of the bubble diameter with respect to the bubble growth time.

According to the force-balance principle, F_{du} can be decomposed to two-component forces as shown in Eqs. (13) and (14).

$$F_{dux} = F_{du}\sin\theta_i \tag{13}$$

$$F_{duy} = F_{du}\cos\theta_i \tag{14}$$

where, θ_i is the bubble inclined angle, which is the angle between the y-axis and the line from the active nucleation site to the bubble center. At the point that bubble lifting off from the heated surface, θ_i can be estimated as zero due to the spherical shape of bubbles.

In Eqs. (11) and (12), $\dot{d}$ refers to the bubble growth rate, which can be simply calculated from the Zuber model (Zuber, 1959). Recently, He et al. (2018) found that the experimental bubble growth rates are proportional to the square root of time, and proposed a new model based on Zuber model. In this study, the bubble growth rate is calculated by Eq. (15).

$$d(t) = C\sqrt{t} \tag{15}$$

where C is an empirical constant related to fluid property, pressure, wall superheat, etc. Zeng et al. (1993) recommended that $C = bJa\sqrt{\kappa_l}$ and $b = 3.904$. Ja is the Jakob Number, $Ja = \rho_l C_{pl}(T_w - T_{sat})/\rho_g h_{lg}$; k_l is the liquid thermal diffusivity rate, $\kappa_l = \lambda_l/\rho_l C_{pl}$, m^2/s; C_{pl} is the liquid specific capacity, J/kg; T_w, T_l, T_{sat} refer to the pipe wall temperature, the liquid temperature, and the liquid saturation temperature, respectively; h_{lg} is the latent heat of vaporization; λ_l is the liquid thermal conductively coefficient, W/(m K). According to Eq. (15), the unstable drag force F_{duy} can be directly calculated.

3.1.6. Surface tension (F_{sy})

This force originates from the contact between the bubble and the heated surface. Klausner et al. (1993) proposed a model to calculate the surface tension between the vapor phase and the liquid phase. Related force on the y-direction is given by Eq. (16).

$$F_{sy} = -d_w\sigma\frac{\pi}{\theta_a - \theta_r}(\cos\theta_r - \cos\theta_a) \tag{16}$$

where θ_r is the bubble receding contact angle; θ_a is the bubble advancing contact angle. In this paper, θ_r and θ_a are $\pi/4$, and $\pi/5$, respectively.

3.1.7. Bubble contact diameter (d_w)

The bubble contact diameter denotes a length of the bubble sticking on the heated surface. However, the value of bubble contact diameter d_w, is hard to be accurately measured since it is difficult to clearly identify the base of the vapor bubble. Lee and Nydahl (1989) stated that the surface tension is one magnitude less than the buoyancy force and the growth force when the bubble is detaching from the pipe wall. Klausner et al. (1993) and Zeng et al. (1993) presented that the bubble contact diameter d_w is approximate to zero at the moment when the bubble detaches from the heated wall. Chen et al. (2012) found that the forces related to the bubble contact diameter (such as surface tension force and contact pressure force) may have the same magnitude as other bubble growing forces. They also revealed that the bubble contact diameter increases with increasing bubble departure diameter, which will affect the bubble lift-off diameters. So, the bubble contact diameter cannot be neglected. In this study, the bubble contact diameter is defined as $d_w = d_b/15$.

3.1.8. Model solution

According to Eqs. (1)–(16), the bubble's force-balance equation on the y-direction can be written by Eq. (17):

$$\frac{1}{6}\pi(\rho_l - \rho_g)g\cos\alpha d_b^3 + \left(\frac{1}{8}C_{sl} + \frac{1}{800}\right)\rho_l u_r^2\pi d_b^2 + \left(\frac{1}{1125}\sigma\pi - \frac{2}{15}\sigma\right)d_b = \frac{1}{8}\rho\pi d^2(t)\left(\frac{3}{2}C_s\dot{d}^2(t) + d(t)\ddot{d}(t)\right) \tag{17}$$

where the bubble growth rate equation $d(t)$ is dependent on the Jakob number and the thermal diffusivity rate. It is suggested to calculated by Eq. (15).

Combining Eqs. (15) and (17) yields a cubic equation in terms of the bubble lift-off diameter as follows:

$$d_b^3 + Bd_b^2 + Cd_b + D = 0 \tag{18}$$

where $B = \frac{\left(\frac{3}{4}C_{sl} + \frac{3}{400}\right)\rho_l u_r^2}{(\rho_l - \rho_g)g\cos\alpha}$, $C = \frac{\left(\frac{2}{375}\sigma\pi - \frac{4}{5}\sigma\right)}{\pi(\rho_l - \rho_g)g\cos\alpha}$, $D = -\frac{3\rho_l b^4 Ja^4\kappa_l^2}{32(\rho_l - \rho_g)g\cos\alpha}$.

If the pipe inclination angle is not equal to 90 degrees ($\alpha \neq \pm 90^\circ$), the bubble lift-off diameter (d_L) can be solved from Eq. (18) by use of the Cardano's Formula, as shown in Eq. (19).

$$\begin{aligned} d_L = &-\frac{B}{3} + \left(\left(-\frac{27D - 9BC + 2B^3}{54}\right)\right. \\ &+ \left(\left(\frac{27D - 9BC + 2B^3}{54}\right)^2 - \left(\frac{3C - B^2}{9}\right)^3\right)^{\frac{1}{2}}\Bigg)^{\frac{1}{3}} \\ &+ \left(\left(-\frac{27D - 9BC + 2B^3}{54}\right) - \left(\left(\frac{27D - 9BC + 2B^3}{54}\right)^2\right.\right. \\ &\left.\left. - \left(\frac{3C - B^2}{9}\right)^3\right)^{\frac{1}{2}}\right)^{\frac{1}{3}} \end{aligned} \tag{19}$$

In particular, the buoyancy force on the y-direction is equal to 0 if the pipe's inclination angle is equal to 90 degrees ($\alpha = \pm 90°$). The bubble lift-off diameter can be calculated from Eq. (20).

$$d_L = \frac{-C \pm \sqrt{C^2 - 4BD}}{2B} \tag{20}$$

The proposed bubble lift-off diameter is summarized as follows: Eq. (19) is applied to calculate the bubble lift-off diameter when $\alpha = \pm 90°$; otherwise, the bubble lift-off diameter is calculated from Eq. (20).

3.2. Existing models

Fritz (1935) firstly proposed a bubble departure diameter correlation for pure liquid based on the balance between the surface tension force and the buoyancy force, as given in Table 1. After

that, Fritz model has been taken as a basement of developing other models. Table 1 lists seven widely used models built from 1935 to 2018. These models have been widely applied to various mixtures.

Kocamustaf and Ishii (1983) introduced a parameter related to the vapor and liquid densities to replace the constant 0.0208 used in the original Fritz model (1935). Zeng et al. (1993) comprehensively investigated the force balance of bubbles in the horizontal boiling blow. They proposed that the relative velocity between the vapor and liquid phases can be ignored. Lee et al. (2003) performed nucleate pool boiling experiments of R11 and R113 on a constant temperature wall surface. Based on experiments, they proposed the Lee model which is a function of the Jakob number, thermal diffusivity, liquid density, and surface tension. Hamzekhani et al. (2014) built a model based on the Buckingham theory and saturated pool boiling experiments of water, ethanol and various binary mixtures, such as ethanol/water, NaCl/water and Na_2SO_4/water over a wide range of concentrations, and. Situ et al. (2005) proposed a correlation based on the force balance principle with consideration of the shear lift force and drag force on the vertical direction. However, the Situ model neglects the bubble contact diameter when bubbles lift from the heated surface. More recently, Chen et al. (2018) proposed an improved Fritz model by use of experimental boiling bubble diameters of ethane.

In comparison with the above seven existing models, the proposed new model considers the unstable drag force in horizontal pipes, the shear lift force and the gas–liquid velocity difference in vertical pipes. Also, the incorporation of the pipe inclination angle enables the new model to calculate the NGL bubble lift-off diameter in various inclined pipes. These improvements contribute to the enhanced accuracy of the proposed model.

4. Results and discussions

In this section, experimental data in vertical and horizontal pipes are collected to validate the accuracy of the new model. The average absolute relative deviation (ARD) between the calculated values and experimental data is defined by Eq. (21) in order to quantitatively evaluate the accuracy of all these models.

$$ARD = \frac{1}{N}\sum_{i=1}^{N}\frac{\left|d_{cali} - d_{exp\,i}\right|}{d_{exp\,i}} \times 100\% \tag{21}$$

where d_{cal} is the calculated bubble lift-off diameter; d_{exp} is the experimental data; N is the total number of data points.

4.1. Model validations for horizontal pipes

Zeng et al. (1993) conducted saturated flow boiling experiments of refrigerant R113. Here, a dataset of 38 experimental data points was applied to validate the new model. These experimental results were also used to evaluate the accuracy of six existing models. All parameters used in the model, including wall superheat, average fluid velocity, heat flux, etc. were set the same values as used by Zeng et al. (1993). Fig. 3 shows the comparisons of experimental bubble lift-off diameters against calculated values based on the new model and existing models with exception of Situ model (Situ et al., 2005), because the Situ model is built for a vertical pipe. If the calculated values are in accordance with the experimental data, all the data points should fall onto the middle slope line. The other two dot lines represent the relative deviation between the calculated lift-off diameter and the experimental value is equal to ±30%. Fig. 3 shows that most of the calculated values based on the new model fall into the scope covered within these two dot lines.

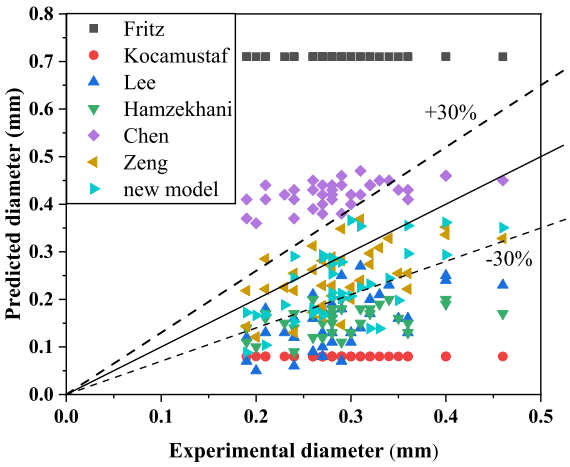

Fig. 3. Comparison of experimental bubble lift-off diameters in horizontal pipes against calculated values based on the new model and six existing models.
Source: Experimental data were taken from Zeng et al. (1993).

The ARD of the new model and six existing models are listed in Table 2. It is calculated that the ARD of the new model is 24.45%, which represents relatively better results in comparison with the other five models except for Zeng model (Zeng et al., 1993). Results reveal that the Zeng model (Zeng et al., 1993) is slightly better than our new model. That is because the Zeng model (Zeng et al., 1993) is specially built based on their experimental data used here as the validation data. Besides, the Fritz model (Fritz, 1935) yields the largest deviation 159.68% because it only accounts for the simple surface tension and buoyancy force but neglects the important drag force acting on the bubble.

4.2. Model validations for vertical pipes

The new model is derived from the theoretical force-balance principle, thus it could be applied to vertical pipes besides horizontal pipes. In this subsection, a total of 28 experimental data points regarding water boiling flow are collected (Okawa et al., 2007) to validate the new model when it is applied to vertical pipes. These experimental data were measured under subcooled conditions rather than saturated flow boiling. That means the only the liquid surrounding the active nucleation site is superheated, and the fluid far away from the site is subcooled. When the growing bubble entries into the subcooled region, it will collapse (Situ et al., 2005). Hence, the effective superheat surrounding the bubble would be less than the wall superheat. We need a new method to calculate the effective superheat. Situ et al. (2005) proposed an effective Jakob number defined by $Ja_e = S\rho_l C_{pl}(T_w - T_{sat})/\rho_g h_{lg}$ to calculate the superheat. In this new model, the suppression factor S is set to 0.8. The other parameters used in model are in accordance with those used by Okawa et al. (2007). The comparisons of experimental bubble lift-off diameters against calculated values based on the new model and six existing models are depicted in Fig. 4. The ARDs of the new model and six existing models are listed in Table 3.

Results demonstrate that the new model yields ARD = 27.95%, which represents the highest accuracy among all the researched models. In particular, the Situ model (Situ et al., 2005) has already been widely used in previous studies. However, the Situ model neglects the contact diameter of the bubble as previously state in Section 3.1.7, resulting in the lower accuracy in this study. Fritz model (Fritz, 1935) and Kocamustaf model (Kocamustaf and Ishii, 1983) only consider surface tension and density, leading

Table 1
Existing models used to calculate the bubble lift-off diameters.

Model	Equation	Forces and influential factors
Fritz (1935)	$d = 0.0208\theta\sqrt{\frac{\sigma}{g(\rho_l-\rho_g)}}$	Surface tension force and buoyancy force
Kocamustaf and Ishii (1983)	$d = 2.64\times10^{-5}\theta\left(\frac{\rho_l-\rho_g}{\rho_g}\right)^{0.9}\sqrt{\frac{\sigma}{(\rho_l-\rho_g)g}}$	Fritz-based model: surface tension force and buoyancy force
Zeng et al. (1993)	$F_b+F_{du}=0F_{du}=-\rho_l\pi r^2\left(\frac{3}{2}C_s\dot{r}^2+r\ddot{r}\right), C_s=\frac{20}{3}$	Drag force and buoyancy force on the horizontal orientation
Lee et al. (2003)	$d=\left(50\sqrt{27}\lambda Ja\sqrt{\frac{\rho_l}{\sigma}}\right)^2$	Dimensionless analysis method
Situ et al. (2005)	$F_{sl}+F_{du}=0,\ d_{lo}^*=\frac{4\sqrt{22/3}b^2}{\pi}Ja^2pr_l^{-1}, b=1.73\ d_{lo}^*=\sqrt{C_l}\left(\frac{u_r d_{lo}}{\upsilon_l}\right)$	Drag force and shear lift force on the vertical direction
Hamzekhani et al. (2014)	$d=KJa^{0.75}\left[\frac{g\rho_l^2}{\mu_l^2}\left(\frac{\sigma}{g\rho_l}\right)^{1.5}\right]^{0.05}\left(\frac{\mu_g q_w}{\sigma\cos\theta\rho_g h_{lg}}\right)^{0.25} K=\sqrt{\frac{\sigma}{(\rho_l-\rho_g)g}}$	Buckingham theory
Chen et al. (2018)	$d=0.3114Ja^{0.315}\sqrt{\frac{\sigma}{(\rho_l-\rho_g)g}}$	Fritz-based model: surface tension force and buoyancy force

Table 2
Absolute relative deviations between experimental lift-off diameters for horizontal pipes and calculated values based on the new model and six existing models.

Model	New model	Fritz	Kocamustaf	Lee	Hamzekhani	Chen	Zeng
ARD, %	24.45	159.68	71.08	46.46	44.88	51.91	19.42

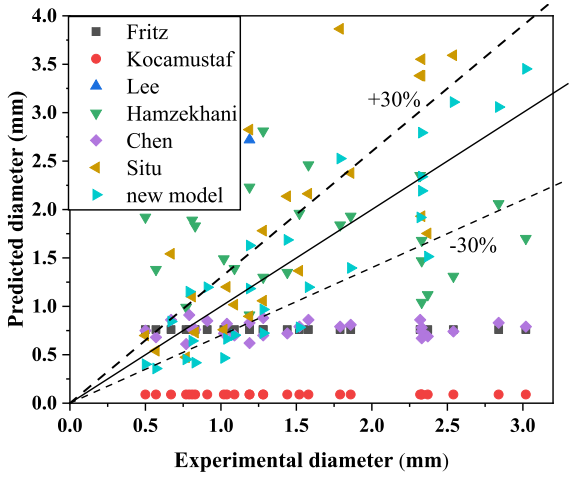

Fig. 4. Comparison of experimental bubble lift-off diameters in vertical pipes against calculated values based on the new model and six existing models.
Source: Experimental data were taken from Okawa et al. (2007).

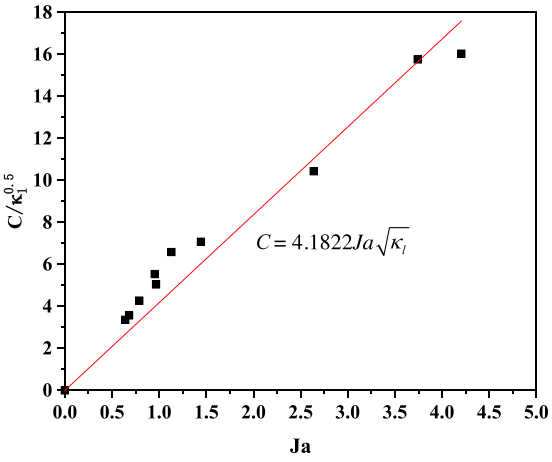

Fig. 5. The linear relationship between Ja and $C/\sqrt{\kappa_l}$.

to larger deviations. Although Lee model (Lee et al., 2003) includes the Jakob number, it still has the largest deviation partly because some coefficients derived from their experiments may not suitable for this study.

4.3. Model validations for NGL fluids

Iso-butane and ethane are common NGL components. The bubble lift-off diameters of iso-butane/ethane have been widely measured in previous studies (Gong et al., 2013; Chen et al., 2004). In the subsection, the measured lift-off diameters are applied to validate the proposed new model as well as existing models given in Table 1. The fluid physical properties involved in the models are calculated from the methods based on the equation of state (Jia et al., 2016; Li et al., 2016; Jia and Okuno, 2018). Some of the physical properties are listed in Tables 4 and 5.

4.3.1. Model validations for Iso-butane

The bubble growth rate is a critical parameter to calculate the bubble lift-off diameter, as expressed by Eqs. (11) to (15). In previous studies (Zuber, 1959; He et al., 2018), the bubble growth rate is assumed to be proportional to the Jakob number and the square root of thermal diffusivity ($C = bJa\sqrt{\kappa_1}$), which indicates that the bubble growth rate is highly related to the thermal properties of the fluid. He et al. (2018) researched the coefficients b and C in the bubble growth equation. They proposed that the Jakob number almost linearly increases with increasing $C/\sqrt{\kappa_l}$ as shown in Fig. 5. The experimental coefficient b then can be calculated from dividing $C/\sqrt{\kappa_l}$ by Ja. According to Fig. 5, the coefficient b is calculated to be 4.1822, which is higher than the value adopted in Zeng Model ($b = 3.09$). However, Eq. (12) shows that the drag force is proportional to the fourth power of the constant b. Hence, increasing the coefficient b will remarkably affect the magnitude of the drag force. In the following cases, the coefficient b = 4.1822 is adopted.

Table 3
Absolute relative deviations between experimental lift-off diameters for vertical pipes and calculated values based on the new model six existing models.

Model	New model	Fritz	Kocamustaf	Lee	Hamzekhani	Chen	Situ
ARD, %	27.95	42.58	92.36	974.67	82.84	43.11	51.2

Table 4
Iso-butane physical properties used to calculate the lift-off diameter.

P/MPa	T/K	Cp/(kJ/kg K)	ρ_g/(kg/m^3)	ρ_l/(kg/m^3)	hlg/(kJ/kg)	σ/(N/M)	λ_l/W/(m K)
0.1	261.07	2.2205	2.7921	594.19	365.4	0.014231	0.10343
0.22	283.06	2.3378	5.8516	569.02	344.71	0.011703	0.09482
0.3	292.91	2.3967	7.8579	557.16	334.58	0.010591	0.091159
0.5	310.86	5.5179	12.877	534.24	314.3	0.008602	0.084824

Table 5
Ethane physical properties used to calculate the lift-off diameter.

P/MPa	T/K	Cp/(kJ/kg K)	ρ_g/(kg/m^3)	ρ_l/(kg/m^3)	hlg/(kJ/kg)	σ/(N/M)	λ_l/W/(m K)
0.1	184.33	2.2205	2.0295	544.13	489.72	0.016231	0.1672
0.3	207.42	2.3967	5.6425	514	456.55	0.012312	0.1458
0.5	220.43	5.5179	9.1568	495.64	434.7	0.010624	0.13421

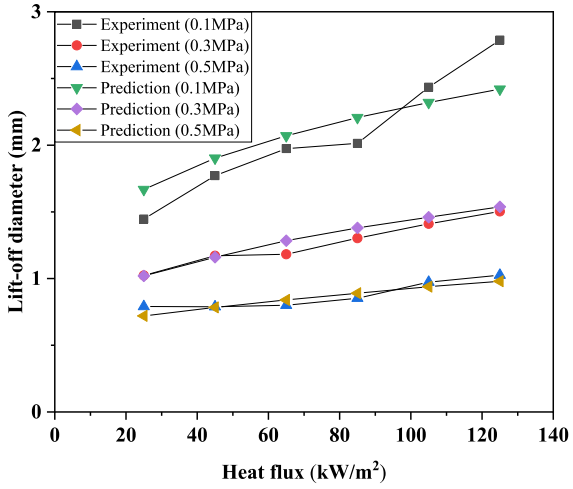

Fig. 6. Comparison of experimental bubble lift-off diameters against calculated values based on the new model at various heat flux.
Source: Experimental data points were taken from Gong et al. (2013).

Gong et al. (2013) measured lift-off diameters of iso-butane boiling flow in horizontal pipes. Fig. 6 shows the comparisons of experimental bubble lift-off diameters against calculated data at different heat flux and pressures based on the new model. Fig. 7(a), (b), and (c) present the comparisons of experimental bubble lift-off diameters at 0.1 MPa, 0.3 MPa, and 0.5 MPa against calculated values based on the new model and six existing models. It is depicted that the new model yields the best results at different pressures. The deviation analysis is listed in Table 6. Results show that the maximum relative deviation of the new model is 9.18% and ARD = 5.73%. Among existing models, the Chen model has the highest accuracy with ARD = 17.08%. These results show that the new model is applicable to iso-butane with considerable accuracy.

Chen et al. (2004) built an experimental apparatus to measure the bubble departure diameters and lift-off diameters of liquid iso-butane boiling on the horizontal surface. The digital images of the bubbles were taken by a high-speed camera from the moment of departure to the lift-off of the bubble. In this subsection, the experimental data are applied to validate the existing models and the new model.

Table 6
Absolute relative deviations between experimental lift-off diameters and calculated values for iso-butane.

Model	Pressure			ARD, %
	0.1 MPa	0.3 MPa	0.5 MPa	
New model	9.18	2.3	4.48	5.75
Fritz	42.45	18.07	12.94	24.49
Kocamustaf	90.91	95.18	96.52	94.21
Lee	458.38	338.31	179.77	325.49
Hamzekhani	27.23	26.46	26.60	26.76
Chen	32.06	23.51	6.39	17.08
Zeng	30.24	26.25	9.93	20.68

Table 7
Absolute relative deviations between experimental lift-off diameters and calculated values for iso-butane.

Model	Pressure		ARD, %
	0.22 MPa	0.30 MPa	
New model	7.82	2.82	5.32
Fritz	14.84	14.6	14.72
Kocamustaf	93.45	94.85	94.15
Lee	344.81	271.19	308.01
Hamzekhani	27.26	34.31	30.78
Chen	9.73	10.33	10.03
Zeng	26.44	12.5	19.47

Fig. 8 shows the comparisons of calculated bubble lift-off diameters against experimental data at different heat flux and pressures. It presents that the lift-off diameter in the horizontal pipeline increases with increasing the heat flux. The calculated results are in accordance with experimental data.

Fig. 9(a) and (b) show the comparisons of experimental data and calculated values at 0.22 MPa and 0.3 MPa respectively. The absolute relative deviations of the new proposed model and existing models are listed in Table 7. It is calculated that the ARD of the new model is 5.32%. Among the existing models, the Chen model (Chen et al., 2018) has the highest accuracy with the ARD = 10.03%. The Lee model (Lee et al., 2003) yields the largest deviation from experimental data with ARD = 308.01%.

4.3.2. Model validations for ethane

The thermophysical properties of ethane are different from those of iso-butane. Hence, the bubble growth model designed for iso-butane is slightly different from ethane. In order to represent the bubble growth process, the coefficient b in the bubble growth

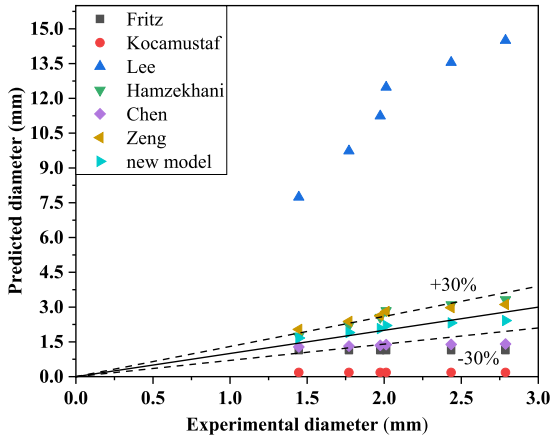

(a) Pressure@0.1MPa

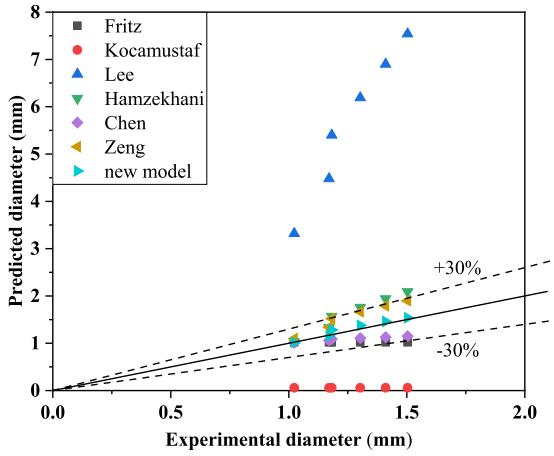

(b) Pressure@0.3MPa

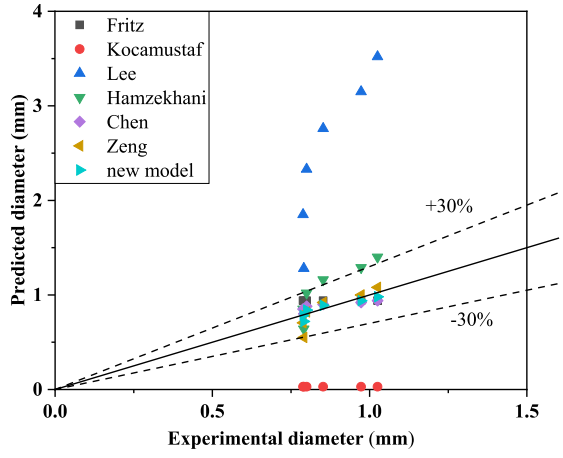

(c) Pressure@0.5MPa

Fig. 7. Comparison of experimental bubble lift-off diameters against calculated values based on the new model and six existing models.
Source: Experimental data points were taken from Gong et al. (2013).

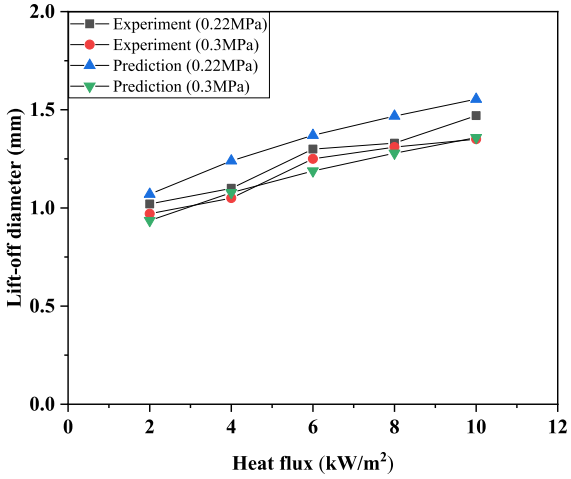

Fig. 8. Comparison of experimental bubble lift-off diameters in horizontal pipes against calculated values based on the new model at various heat flux and pressures.
Source: Experimental data were taken from Chen et al. (2004).

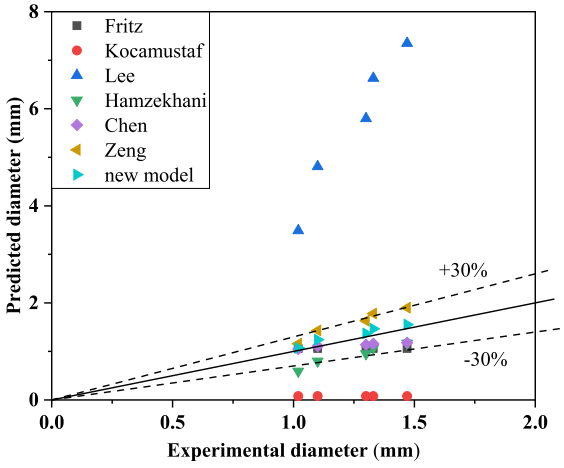

(a) Pressure@0.22MPa

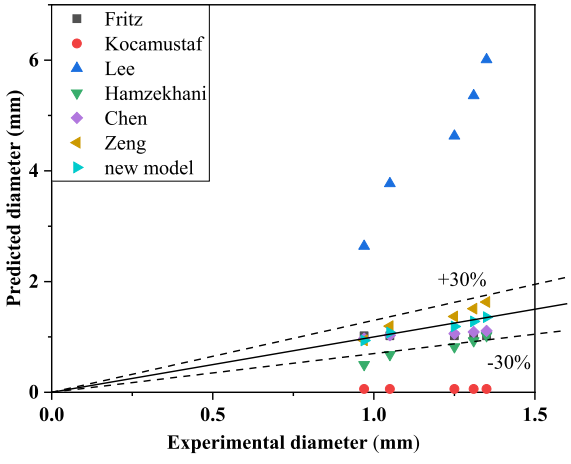

(b) Pressure@0.3MPa

Fig. 9. Comparison of experimental bubble lift-off diameters in horizontal pipes against calculated values based on the new model and seven existing models.
Source: Experimental data were taken from Chen et al. (2004).

Table 8
Absolute relative deviations between experimental lift-off diameters and calculated values for ethane of Gong dataset.

Model	ARD, %			Overall ARD, %
	0.1 MPa	0.3 MPa	0.5 MPa	
New model	18.38	6.78	1.96	9.04
Fritz	56.72	22.64	15.33	31.56
Kocamustaf	91.48	94.66	95.75	93.96
Lee	470.42	263.05	171.80	301.76
Hamzekhani	18.35	12.33	17.51	16.06
Chen	51.35	26.68	19.14	32.39
Zeng	21.59	16.51	28.50	22.2

model for ethane is set to 5.6. Gong et al. (2013) measured lift-off diameters of ethane in horizontal pipes. Comparisons of experimental data and calculated values at 0.1MPa, 0.3MPa, and 0.5MPa are shown in Fig. 10(a), (b), and (c), respectively. Fig. 11 depicts comparisons of calculated bubble lift-off diameters against experimental data at different heat flux and pressures. The deviation analysis is listed in Table 8. Results demonstrate that the new model has the highest accuracy with overall ARD = 9.04%.

4.4. Effects of parameters on the bubble lift-off diameters

The bubble lift-off diameter depends on many parameters including the bubble shape parameters and the pipe operation parameters, such as the bubble's advancing and receding contact angles (α and β), wall contact diameter (d_w), pipeline inclination angle, pressure, temperature, flow velocity, wall heat flux, etc. As one of the most important parameters, the effects of the pipe inclination angle on the bubble lift-off diameter is researched. Besides, the Jakob number is a comprehensive parameter that incorporates the fluid properties and heat flux. So, the effects of the Jakob number are also researched in what follows.

4.4.1. Effects of the pipe inclination angle

The new bubble lift-off model has theoretically derived from the bubble force-balance principle at different inclination angles. Hence, besides horizontal and vertical pipes, this new model can be extended to pipes with arbitrary inclination angles. In this subsection, this new model is applied to calculate the bubble lift-off diameters in pipes with inclination angles from 0 to 90 degrees, as well as the heat flux from 25 kW/m^2 to 125 kW/m^2. The results are shown in Fig. 12.

Fig. 12 demonstrates that the new model is able to continuously predict the bubble lift-off diameters in pipes with varies inclination angles, which represents a significant improvement in comparison with existing models given in Table 1. In addition, Fig. 12 demonstrates that the lift-off diameter increases with increasing the pipe inclination angle.

Fig. 13 depicts the variations of all the forces with the bubble diameter in horizontal pipes. The bubble will lift off from the heated wall when the summation of all the forces acting on the bubble is higher than zero. It is shown that, for the horizontal pipe, the summation of force is dominated by the shear lift force (F_{sl}), buoyancy force (F_{by}), drag force (F_{duy}) and surface tension force (F_{sy}). The drag force and surface tension force are negative values, which tend to keep the bubble staying on a heated wall. In contrast, the shear lift force and buoyancy force are positive values, which tend to take the bubble away from the heated wall. Once the summation of forces expressed by Eq. (1) is higher than zero, the bubble lifts from the wall.

Unlike the horizontal pipes, the y-component of the buoyancy force acting on bubbles is equal to zero for the vertical pipe. The dominated forces that affect the bubble lift-off diameter are the shear lift force (F_{sl}), drag force (F_{duy}) and surface tension force (F_{sy}). The absence of the buoyancy force will result in the prolongation of the bubble growth time on the heated wall. Finally, the

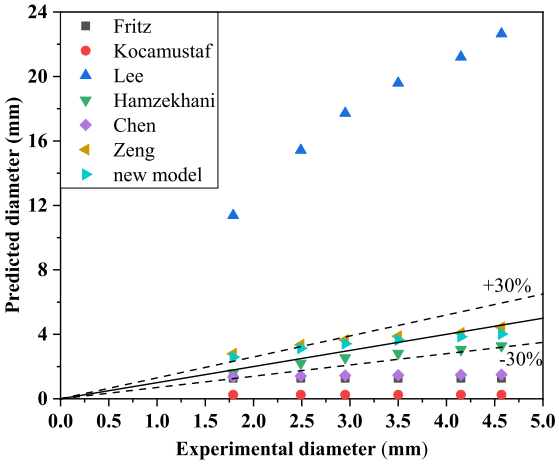

(a) Pressure@0.1MPa

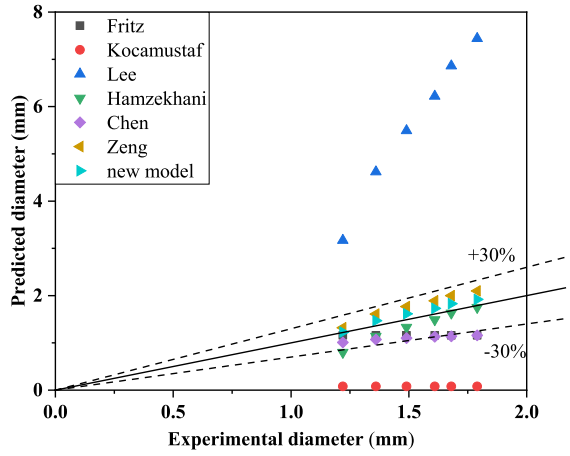

(b) Pressure@0.3MPa

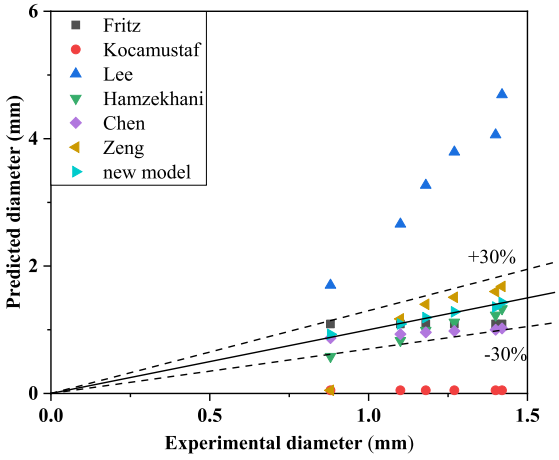

(c) Pressure@0.5MPa

Fig. 10. Comparison of experimental ethane lift-off diameters against calculated values based on the new model and six ting models.
Source: Experimental data points were taken from Gong et al. (2013).

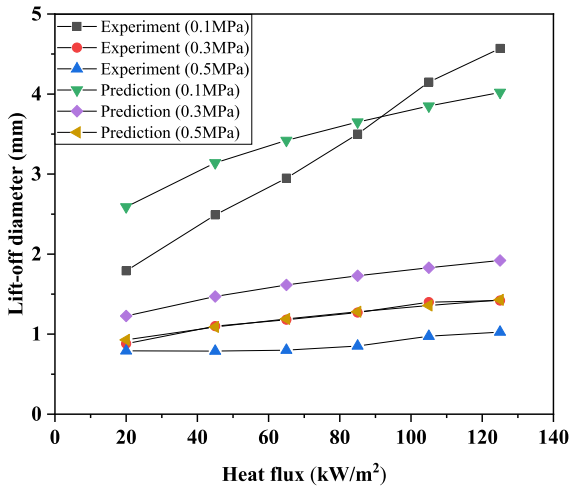

Fig. 11. Comparison of experimental ethane lift-off diameters against calculated values at different heat flux.
Source: Experimental data points were taken from Gong et al. (2013).

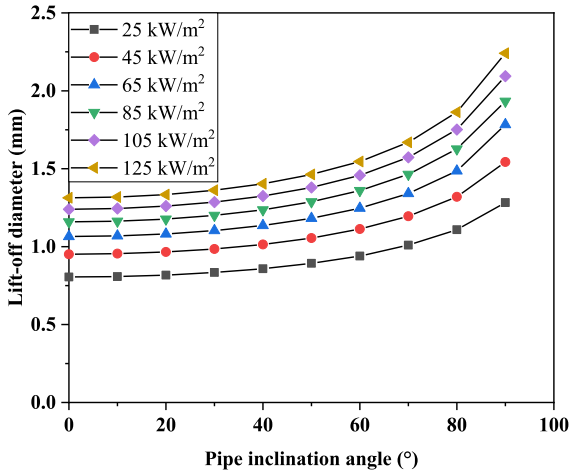

Fig. 12. The calculated bubble lift-off diameters at different pipe inclination angles and heat flux for Iso-butane; P = 0.3 MPa, u = 0.5 m/s.

increased bubble growth time results in an increase of the bubble lift-off diameter.

Results demonstrate that all the forces proposed in this paper, in particular the shear lift force (F_{sl}), buoyancy force (F_{by}), drag force (F_{duy}) and surface tension force (F_{sy}) should be considered in order to accurately calculate the bubble lift-off diameter. Previous models do not cover these essential four forces, resulting in relatively poor results when they are applied to the above cases. For example, the Fritz-based model (Fritz, 1935; Kocamustaf and Ishii, 1983; Chen et al., 2018) only consider the surface tension force and buoyancy force; Zeng model (Zeng et al., 1993) only accounts for the Drag force and buoyancy force on the horizontal orientation; Situ model (Situ et al., 2005) is built based on the balance between the drag force and shear lift force on vertical orientation. Besides, the Lee model (Lee et al., 2003) is built based on the dimensionless analysis method, and the Hamzekhani model (Hamzekhani et al., 2014) is developed based on the Buckingham theory. These results show that the new model built based on the force-principle method has higher accuracy in comparison with these two theory-based methods.

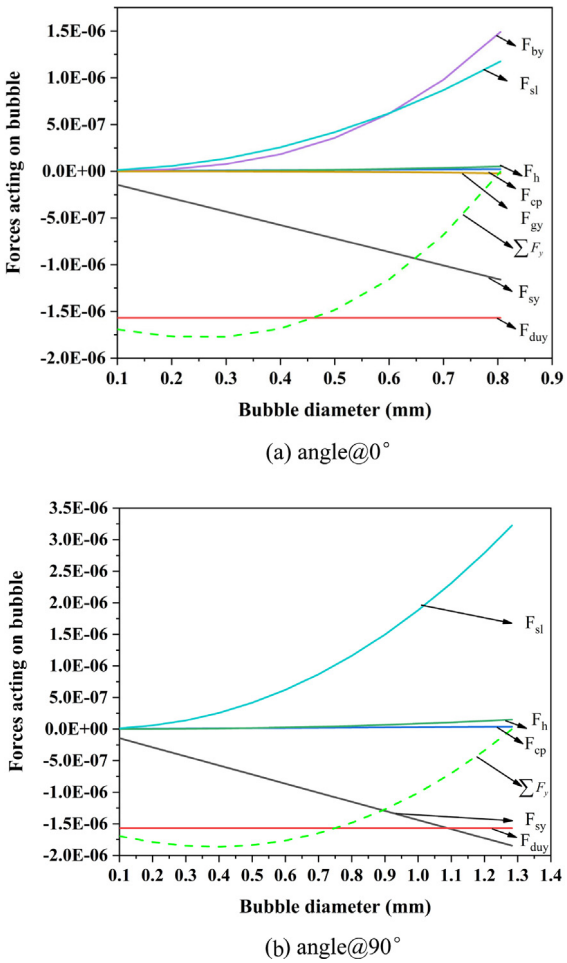

Fig. 13. Variation of all the forces with the bubble diameter. These results are calculated for horizontal and vertical pipes for iso-butane. P = 0.3 MPa, u = 0.5 m/s.

4.4.2. Effects of the Jakob number

The Jacob number is a comprehensive number related to the fluid properties, pipe wall temperature, and superheat. Fig. 14 represents that the bubble lift-off diameter almost linearly increases with increasing the Jakob number. Eq. (15) presents that the increase of the Jakob number directly increases the bubble growth rate, which finally increases the bubble lift-off diameter.

5. Conclusions

This paper built a new lift-off diameter model for boiling bubbles in natural gas liquids transmission pipelines based on the force-balance principles. The main conclusions are summarized as follows:

(1) The new bubble lift-off model considers the effects of the pressure, shear lift force, unstable drag force, surface tension, gravity force, buoyancy force, gas-phase density, bubble volume, bubble flow velocity, and bubble growth time on the bubble lift-off diameters at different pipe inclination angles. The new model can continuously calculate the bubble lift-off diameter in pipes with various inclination angles from horizontal to vertical, overcoming the deficiencies of most existing models that only can be applied to horizontal and vertical pipes.

(2) A total of 136 data points collected from the literature were applied to validate the new model. For horizontal and vertical

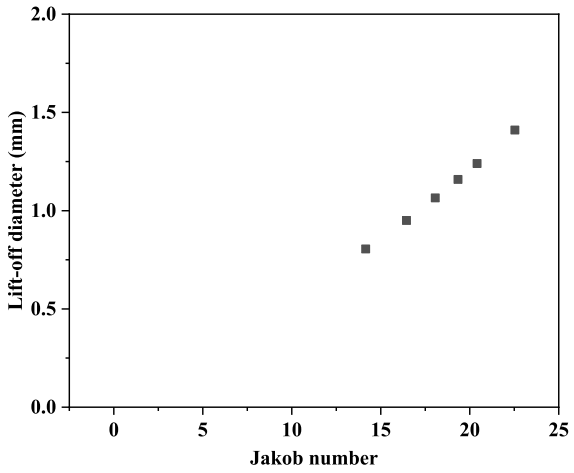

Fig. 14. Effect of Jakob number on bubble lift-off diameter for Iso-butane, 0.3 MPa, u = 0.5 m/s.

pipes, the average relative deviations (ARD) between the experimental bubble lift-off diameters and calculated values based on the new model are equal to 24.45% and 29.95%, respectively. For iso-butane and ethane pipes, a new modification method regarding the Jacob number-related coefficient is proposed to match the experimental data and calculated values. As a result, the ARDs of the new model for iso-butane and ethane pipes are equal to 5.75% and 9.04%, respectively. Results demonstrate that the new model is superior to the other seven existing models, including the Fritz, Kocamustaf, Zeng, Lee, Situ, Hamzekhani, Chen models.

(3) Results demonstrate that, for inclined pipes, the shear lift force (F_{sl}), buoyancy force (F_{by}), drag force (F_{duy}) and surface tension force (F_{sy}) are dominant factors affecting the bubble lift-off diameter, which provides research directions to improve existing models that are designed for other fluids. The improvements regarding the new model will further contribute to the accurate hydraulic and thermal simulation of NGL transmission pipelines.

Declaration of competing interest

The authors declare that they have no known competing financial interests or personal relationships that could have appeared to influence the work reported in this paper.

CRediT authorship contribution statement

Wenlong Jia: Conceptualization, Methodology, Validation, Investigation, Resources, Writing - original draft, Writing - review & editing, Visualization. **Youzhi Lin:** Validation, Investigation, Formal analysis, Writing - review & editing, Visualization. **Fan Yang:** Validation, Investigation, Writing - original draft. **Changjun Li:** Project administration, Funding acquisition, Writing - review & editing, Supervision.

Acknowledgments

This study was financially supported by the National Natural Science Foundation of China (No. 51604233, No. 51674213, No. 51974269), a sub-project of the National Science and Technology Major Project of China (No. 2016ZX05028-001-006).

References

Chen, Y., Groll, M., Mertz, R., Kulenovic, R., 2004. Bubble dynamics of boiling of propane and iso-butane on smooth and enhanced tubes. Exp. Therm. Fluid Sci. 28, 171–178. http://dx.doi.org/10.1016/S0894-1777(03)00036-0.

Chen, D., Pan, L.-m., Ren, S., 2012. Prediction of bubble detachment diameter in flow boiling based on force analysis. Nucl. Eng. Des. 243, 263–271. http://dx.doi.org/10.1016/j.nucengdes.2011.11.022.

Chen, H., Yao, Y., Gong, M., 2018. Experimental study on bubble departure diameter of ethane saturated nucleate pool boiling. CIESC J. 64, 1419–1427. http://dx.doi.org/10.11949/j.issn.0438-1157.20170802.

Cho, Y.-J., Yum, S.-B., Lee, J.-H., Park, G.-C., 2011. Development of bubble departure and lift-off diameter models in low heat flux and low flow velocity conditions. Int. J. Heat Mass Transfer 54, 3234–3244. http://dx.doi.org/10.1016/j.ijheatmasstransfer.2011.04.007.

Cole, R., Rohsenow, W.M., 1969. Correlation of bubble departure diameters for boiling of saturated liquids. Chem. Eng. Prog. 65.

Colombo, M., Fairweather, M., 2015. Prediction of bubble departure in forced convection boiling: A mechanistic model. Int. J. Heat Mass Transf. http://dx.doi.org/10.1016/j.ijheatmasstransfer.2015.01.103.

Faraji, D., Barnea, Y., Salcudean, M., 1994. Visualization study of vapor bubbles in convective subcooled boiling of water at atmospheric pressure. Rev. Esp. Cardiol. 425–430. http://dx.doi.org/10.1615/IHTC10.1230.

Fritz, W., 1935. Berechnungen des Maximalvolumens von Dampfblasen. Physica Z.

Gong, M., Wu, Y., Ding, L., Cheng, K., Wu, J., 2013. Visualization study on nucleate pool boiling of ethane, isobutane and their binary mixtures. Exp. Therm. Fluid Sci. 51, 164–173. http://dx.doi.org/10.1016/j.expthermflusci.2013.07.011.

Hamzekhani, S., Maniavi Falahieh, M., Akbari, A., 2014. Bubble departure diameter in nucleate pool boiling at saturation: Pure liquids and binary mixtures. Int. J. Refrig. 46, 50–58. http://dx.doi.org/10.1016/j.ijrefrig.2014.07.003.

He, J., Liu, J., Xu, X., 2018. Experimental investigation of single bubble growth in the boiling of the superheated liquid mixed refrigerants. Int. J. Heat Mass Transfer 127, 553–565. http://dx.doi.org/10.1016/j.ijheatmasstransfer.2018.06.045.

Jia, W., Li, Z., Liao, K., Li, C., 2016. Using Lee–Kesler equation of state to compute the compressibility factor of CO_2 -content natural gas. J. Nat. Gas Sci. Eng. http://dx.doi.org/10.1016/j.jngse.2016.07.032.

Jia, W., Okuno, R., 2018. Modeling of asphaltene and water associations in petroleum reservoir fluids using cubic-plus-association EOS. AIChE J. http://dx.doi.org/10.1002/aic.16191.

Jia, W., Wu, X., C, L.I., He, Y., 2017. Characteristic analysis of a non-equilibrium thermodynamic two-fluid model for natural gas liquid pipe flow. J. Nat. Gas Sci. Eng. 40, 132–140. http://dx.doi.org/10.1016/j.jngse.2016.07.032.

Jia, W., Yang, F., Wu, X., Li, C., Wang, Y., 2020. Predictions on temperatures of high-pressure gas/water/MEG mixtures flowing through wellhead chokes. J. Nat. Gas Sci. Eng. 74, 103108. http://dx.doi.org/10.1016/j.jngse.2019.103108.

Kim, J., Kim, M.H., 2006. On the departure behaviors of bubble at nucleate pool boiling. Int. J. Multiph. Flow 32, 1269–1286. http://dx.doi.org/10.1016/j.ijmultiphaseflow.2006.06.010.

Kirichenko, Y., 1973. Evaluation of the conditions of vapor bubble separation during nucleate boiling. J. Eng. Phys. 25, 811–817. http://dx.doi.org/10.1007/BF00829587.

Kirichenko, I., Dolgoi, M., Levchenko, N., Tsybulskii, V., Slobozhanin, L., Shcherbakova, N., 1976. The boiling of cryogenic liquids. Heat Transf. Sov. Res. 8.

Klausner, J., Mei, R., Bernhard, D.M., Zeng, L.Z., 1993. Vapor bubble departure in forced convection boiling. Int. J. Heat Mass Transfer 36, 651–662. http://dx.doi.org/10.1016/0017-9310(93)80041-R.

Kocamustaf, G., Ishii, M., 1983. Interfacial area and nucleation site density in boiling systems. Int. J. Heat Mass Transfer 26, 1377–1387. http://dx.doi.org/10.1016/S0017-9310(83)80069-6.

Lee, R., Nydahl, J., 1989. Numerical calculation of bubble growth in nucleate boiling from inception through departure. J. Heat Transf.-Trans. ASME http://dx.doi.org/10.1115/1.3250701.

Lee, H., Oh, B., Bae, S., Kim, M.H., 2003. Single bubble growth in saturated pool boiling on a constant wall temperature surface. Int. J. Multiph. Flow 29, 1857–1874. http://dx.doi.org/10.1016/j.ijmultiphaseflow.2003.09.003.

Li, Z., Jia, W., Li, C., 2016. An improved PR equation of state for CO_2-containing gas compressibility factor calculation. J. Nat. Gas Sci. Eng. http://dx.doi.org/10.1016/j.jngse.2016.11.016.

Mei, R., Klausner, J., 1994. Shear lift force on spherical bubbles. Int. J. Heat Fluid Flow 15, 62–65. http://dx.doi.org/10.1016/0142-727X(94)90031-0.

Okawa, T., Kubota, H., Ishida, T., 2007. Simultaneous measurement of void fraction and fundamental bubble parameters in subcooled flow boiling. Nucl. Eng. Des. 237, 1016–1024.

Saffman, P., 1965. The lift on a small sphere in a slow shear. J. Fluid Mech. 22, 385–400. http://dx.doi.org/10.1017/S0022112065000824.

Shao, X.F., Li, X., Wang, R.-S., 2011. Numerical simulation of liquid nitrogen boiling flow in vertical annular pipe. Chem. Eng. 39, 82–86+95.

Situ, R., Hibiki, T., Ishii, M., Mori, M., 2005. Bubble lift-off size in forced convective subcooled boiling flow. Int. J. Heat Mass Transf. http://dx.doi.org/10.1016/j.ijheatmasstransfer.2005.06.031.

Stevens, P., 2012. The 'Shale Gas Revolution': Developments and Changes. Chatham House, London.

Torregrosa, A., Broatch, A., Olmeda, P., Cornejo, O., 2016. A note on bubble sizes in subcooled flow boiling at low velocities in internal combustion engine-like conditions. J. Appl. Fluid Mech. 9, 2321–2332. http://dx.doi.org/10.18869/acadpub.jafm.68.236.23211.

Wang, Z.Y., Luo, D.K., Liu, L.L., 2018. Natural gas utilization in China: Development trends and prospects. Energy Rep. 4, 351–356.

Zeng, L.Z., Klausner, J., Mei, R., 1993. A unified model for the prediction of bubble detachment diameters in boiling systems— I. Pool boiling. Int. J. Heat Mass Transfer 36, 2261–2270. http://dx.doi.org/10.1016/S0017-9310(05)80111-5.

Zuber, N., 1959. Hydrodynamic Aspects of Boiling Heat Transfer. Atomic Energy Commission Report, http://dx.doi.org/10.2172/4175511.